SUPPLEMENTARY MATERIAL

Capillary Electrophoresis with Laser-Induced Fluorescent Detection of Immunolabeled Individual Autophagy Organelles Isolated from Tissue

Katherine A. Muratore,[1] Heather M. Grundhofer,[2] and Edgar A. Arriaga[2*]

University of Minnesota, Twin Cities

[1]Department of Biochemistry, Molecular Biology, and Biophysics, 321 Church St SE, Minneapolis, MN 55455

[2]Department of Chemistry, 207 Pleasant St SE, Minneapolis, MN 55455

*Corresponding Author

TABLE OF CONTENTS

.

Supplementary Methods

Immunoblotting. Tris buffered saline, (TBS, 10 × concentration, 200nM Tris, 5M NaCl, pH 7.4), Tween-20, goat anti rabbit IgG: HRP, and 15% Tris-HCl Precast SDS-Page gels were obtained from Bio-Rad (Hercules, CA). Dylight488 conjugated rabbit anti-LC3 antibody, unconjugated rabbit anti-LC3 antibody, and rabbit anti-ATG5 antibody were obtained from Novus Biologicals (Littleton, CO). Skim milk powder was obtained from Wal-Mart (Bentonville, AR). Rabbit anti-GAPDH antibody was obtained from Rockland Immunochemical (Pottstown, PA). ATG5 (-/-) and (+/+) MEFS whole cell lysates were fractionated by 15% SDS-PAGE using a Criterion Cell apparatus (Bio-Rad). Gels were transferred to 0.45µm nitrocellulose membrane (Bio-Rad) using a Criterion Blotter apparatus (Bio-Rad). Membranes were blocked in 5% skim milk in TBS, 0.5% Tween-20. Membranes were probed overnight with 1:500 anti-ATG5, 1:5000 anti-GAPDH, and 1:1000 anti-LC3 primary antibody dilutions in 4% skim milk in TBS, 0.5% Tween-20. Secondary antibodies were goat anti rabbit IgG:HRP. All washes were with TBS, 0.5% Tween-20. The final washed blots were visualized on X-ray film using Pierce Super Signal West Femto substrate (Thermo Fisher Scientific). Films were digitized using a scanner and converted to 16-bit grayscale using ImageJ 1.51d (NIH, Bethesda, MD). Densitometry analysis was also performed in ImageJ.

Quantitative real-time PCR. Quantitative real-time PCR. The levels of ATG5 mRNA in ATG5 KO and WT MEFs were quantified using primers that amplify bases 242 to 341of ATG5 transcript variant 1 (NM.053069.6). RNA was isolated from ATG5 KO and WT MEFs using Trizol (Trizol Plus RNA Purification Kit, Thermo Fischer Scientific), followed by a DNAse treatment to rid samples of contaminating genomic DNA (RNAse-Free DNAse Set, RNeasy MinElute Kit, Qiagen). Single-strand cDNA was synthesized with oligo(dT) primers using AffinityScript Multiple Temperature Reverse Transcriptase (Agilent AffinityScript QPCR cDNA Synthesis Kit) and 5 ng of total RNA as template. Real-time analysis was performed using the Mx3000P QPCR System (Agilent) with the synthesized cDNA and Brilliant II SYBR Green PCR Master Mix (Agilent). Quantification of specific mRNA levels was calculated relative to the reference gene ACTB, using the comparative C_T method. A single dominant post-amplification product was confirmed via melting curves and agarose gel electrophoresis (single band corresponding to 100 or 188 bases for ATG5 or ACTB, respectively). Measured amplification efficiencies of both the ATG5 and ACTB amplicons were comparable, validating our use of the comparative C_T method. All reactions were run in triplicate and values are reported as mean ± SEM.

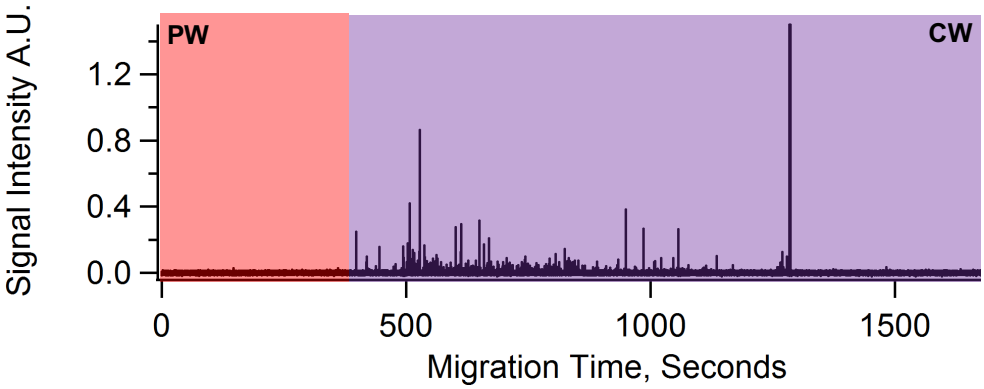

Supplementary Figure 1. False Positive Rate. The electropherogram (CE-LIF) or flowgram (capillary cytometry) are divided into "premigration" (PW) and "collection" (CW) windows. Equation 1 of the main text, uses the length of time it takes for the first organelle to reach the detector (P), the length of time where organelles are detected (W), the number of events (N) that occur during the PW, which are considered false positives, and the number of events (O_T) observed in the CW, which includes both false and true positives. Equation 1, assumes that the rate of false positives remains constant throughout the PW and CW. In the example electropherogram above, P = 418s, W = 1262s, N = 3 events, and O_T = 278 events. Equation 1 predicts that the number of true positives (O_C) is 269.

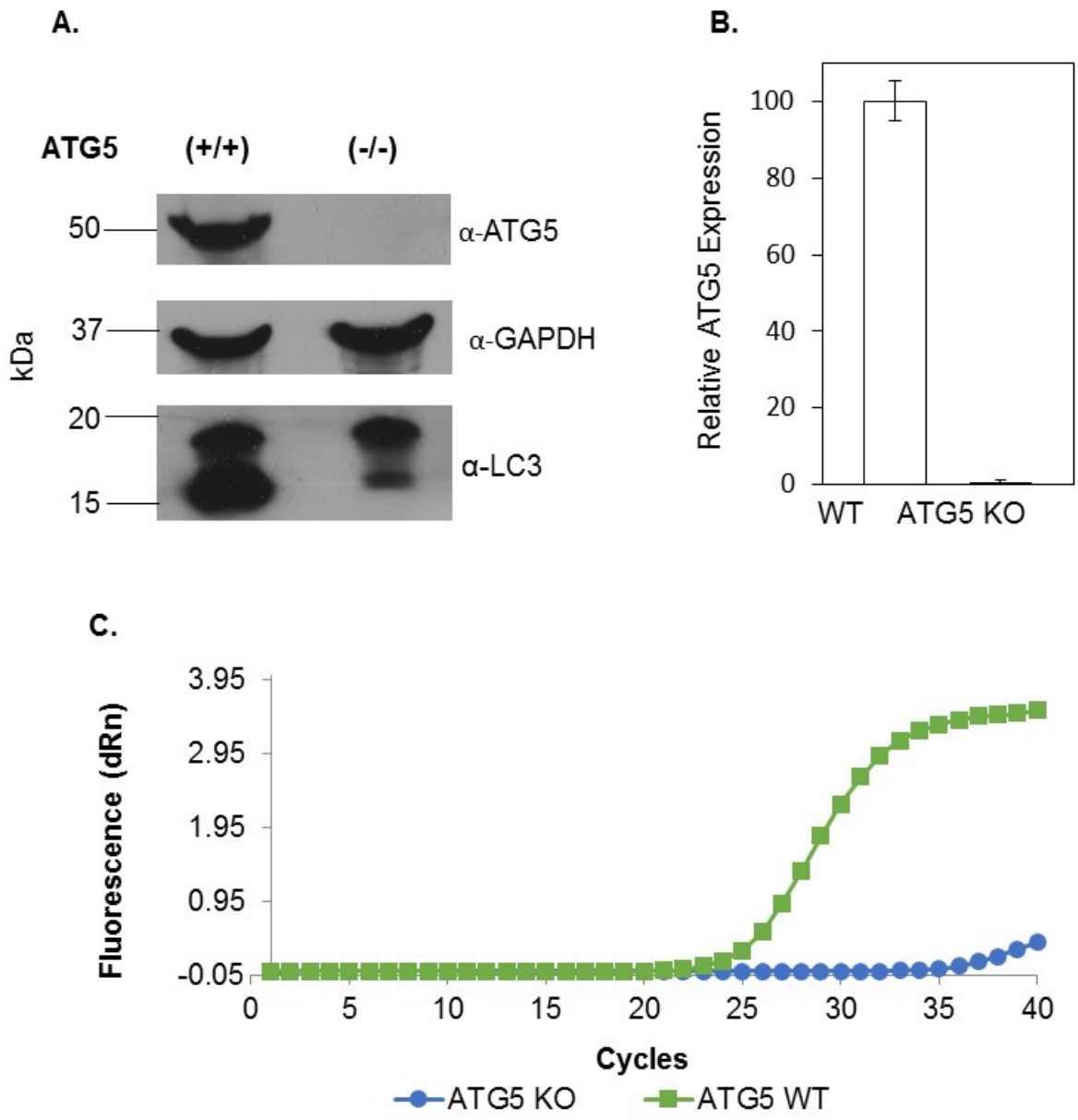

Supplementary Figure 2. Validation of wild type ATG5 (*+/+)* and knock-out ATG5 (*-/-)* MEFs. (A) Cell extracts were subject to separate blots probed independently with rabbit anti-ATG5, rabbit anti-GAPDH, or rabbit anti-LC3 antibodies. All lanes were loaded with 8µg protein. Positions of molecular mass markers are indicated on the left side. For ATG5 (+/+), S/N ~13,000; minimum amount of protein needed for detection ~ 15 fg. (B) ATG5 mRNA levels in the knock-out (ATG5 KO) and Wild type ATG5 (WT) MEFS were determined by qRT-PCR. Normalized data are means +/- SEM (n=3). The following primer sequences were used to assess ATG5 and ACTB mRNA levels: *ATG5* sense CTC GGT TTG GCT TTG GTT GA and antisense ACC ACA CAT CTC GAA GCA CA; *ACTB* sense AGG TGA CAG CAT TGC TTC TG and antisense GCT GCC TCA ACA CCT CAA C. (C) Representative amplification plot from qPCR reaction.

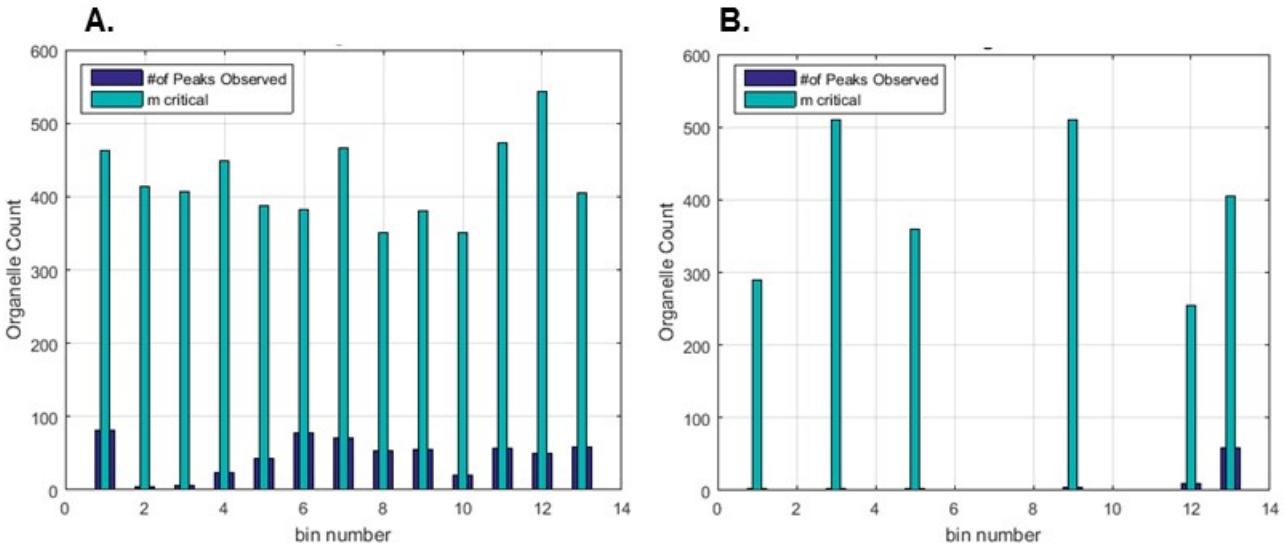

Supplementary Figure 3. **Statistical overlap theory of autophagy organelles from ATG5 (+/+) and *(-/-)* MEFS labeled with 300nM DyLight488-conjugated anti-LC3 antibody**. (A) Organelle counts for ATG5 (+/+). (B) Organelle counts for ATG5 (-/-) data. CE-LIF data was partitioned into bins of a consistent length, and the threshold saturation value was estimated based on the bin length in seconds, average peak width, and number of bins. The threshold saturation value is represented as m critical in the bar graph. For more information see Figure 2 in the main manuscript.

.

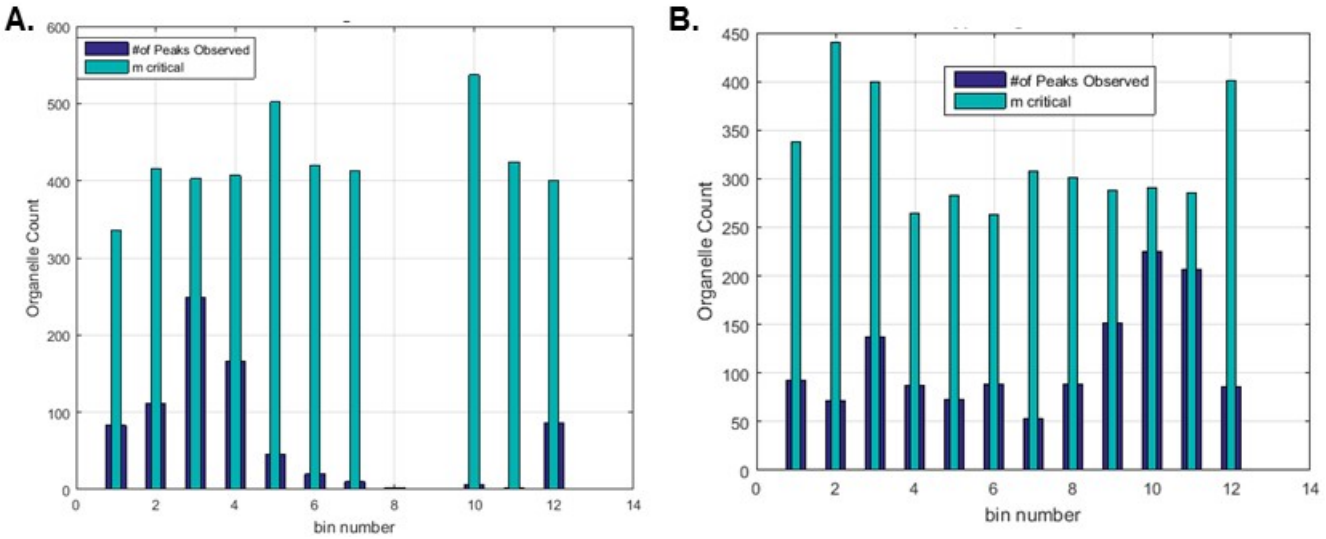

Supplementary Figure 4. **Statistical overlap theory of autophagy organelles from murine liver tissue labeled with 300nM DyLight488-conjugated anti-LC3 antibody and Dylight488-conjugated Isotype control.** (A) Organelle counts for labeling with DyLight488-conjugated anti-LC3 antibody. (B)) Organelle counts for labeling with DyLight488-conjugated isotype control. Other conditions were as described in Figure S2. For more information see Figure 3 in the main manuscript.

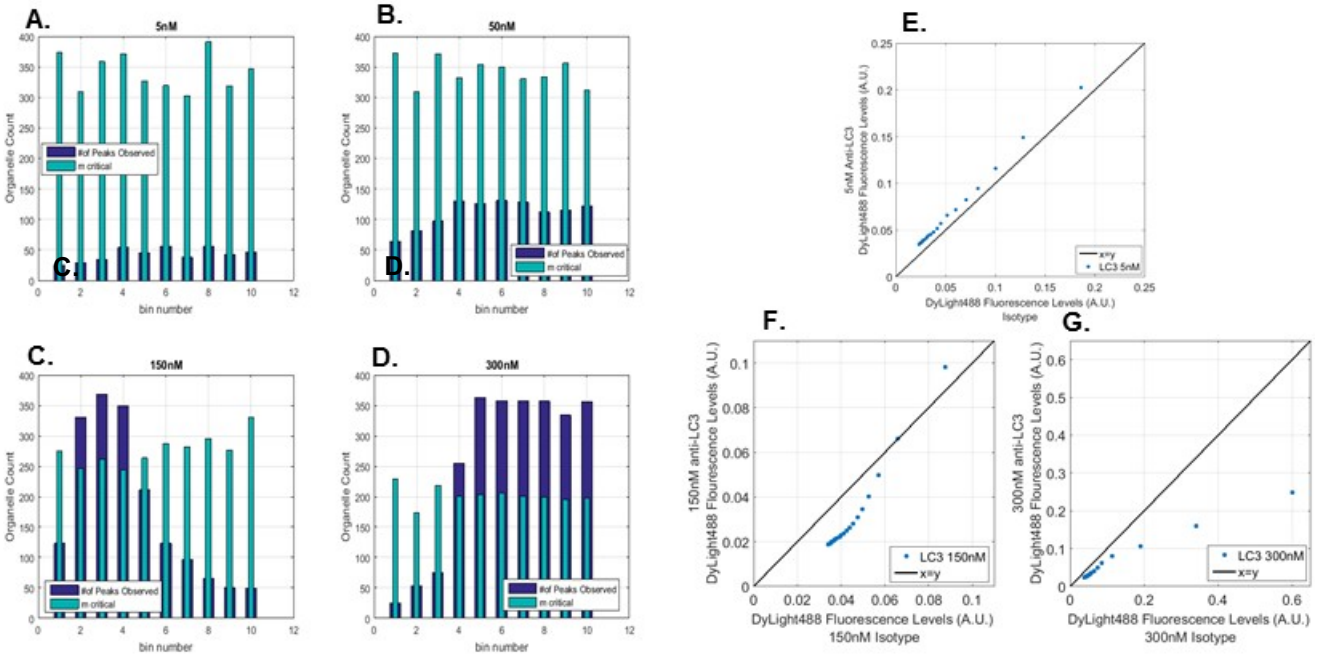

Supplementary Figure 5. Statistical overlap theory and QQ plot analysis of autophagy organelles from murine liver tissue labeled with 5-300nM DyLight488-conjugated anti-LC3 antibody. (A-D) Statistical overlap theory of autophagy organelles from murine liver tissue labeled with (A) 5nM, (B) 50nM, (C) 150nM, or (D) 300nM DyLight488 anti-LC3. Other conditions were as described in Figure S2. There were severe SOT violations when using 150 nM (C) and 300 nM (D) antibody concentrations. Elimination of compromised bins results in 59% and 94% reduction, respectively, in the number of organelles that are representative of individual events. (E-G) QQ plots to compare intensity distributions from anti-LC3 antibody and isotype control. The intensity percentiles from 5nM (E), 150nM (F), and 300nM (G) anti-LC3 labeled sample (y-axis) are plotted against the intensity percentiles from the isotype labeled sample (x axis). Data from 150 nM and 300 nM exclude data with SOT violations represented in (C) and (D), respectively. For more information see Figure 4 in the main manuscript.

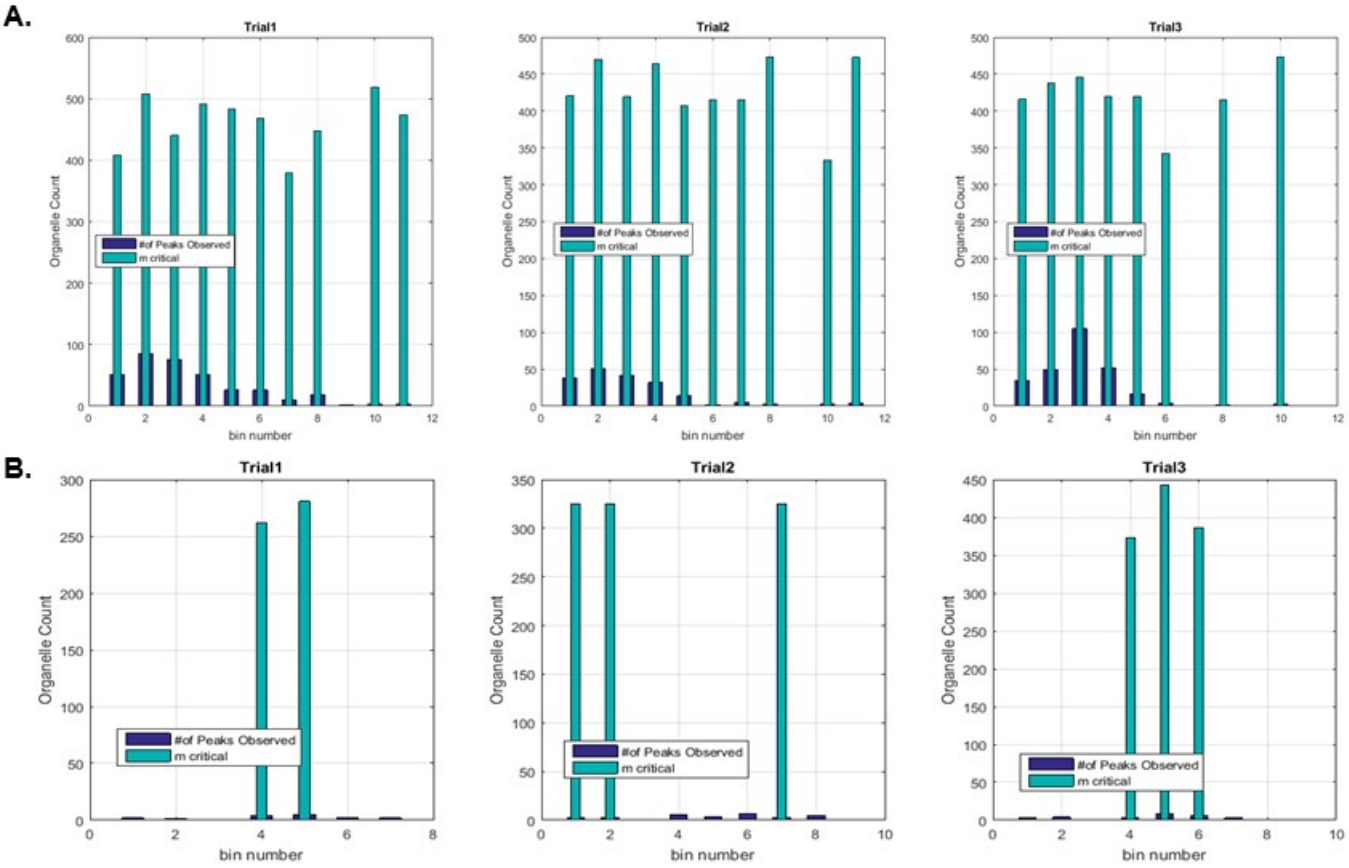

Supplementary Figure 6. **Statistical overlap theory of autophagy organelles from murine liver tissue labeled with 50nM DyLight 488-conjugated anti-LC3 antibody or 50nM DyLight 488-conjugated isotype control.** (A) Organelle counts for DyLight 488-conjugated anti-LC3 antibody. (B) Organelle counts for DyLight 488-conjugated isotype control. Other conditions were as described in Figure S2. Data correspond to Figure 5 of the main manuscript.

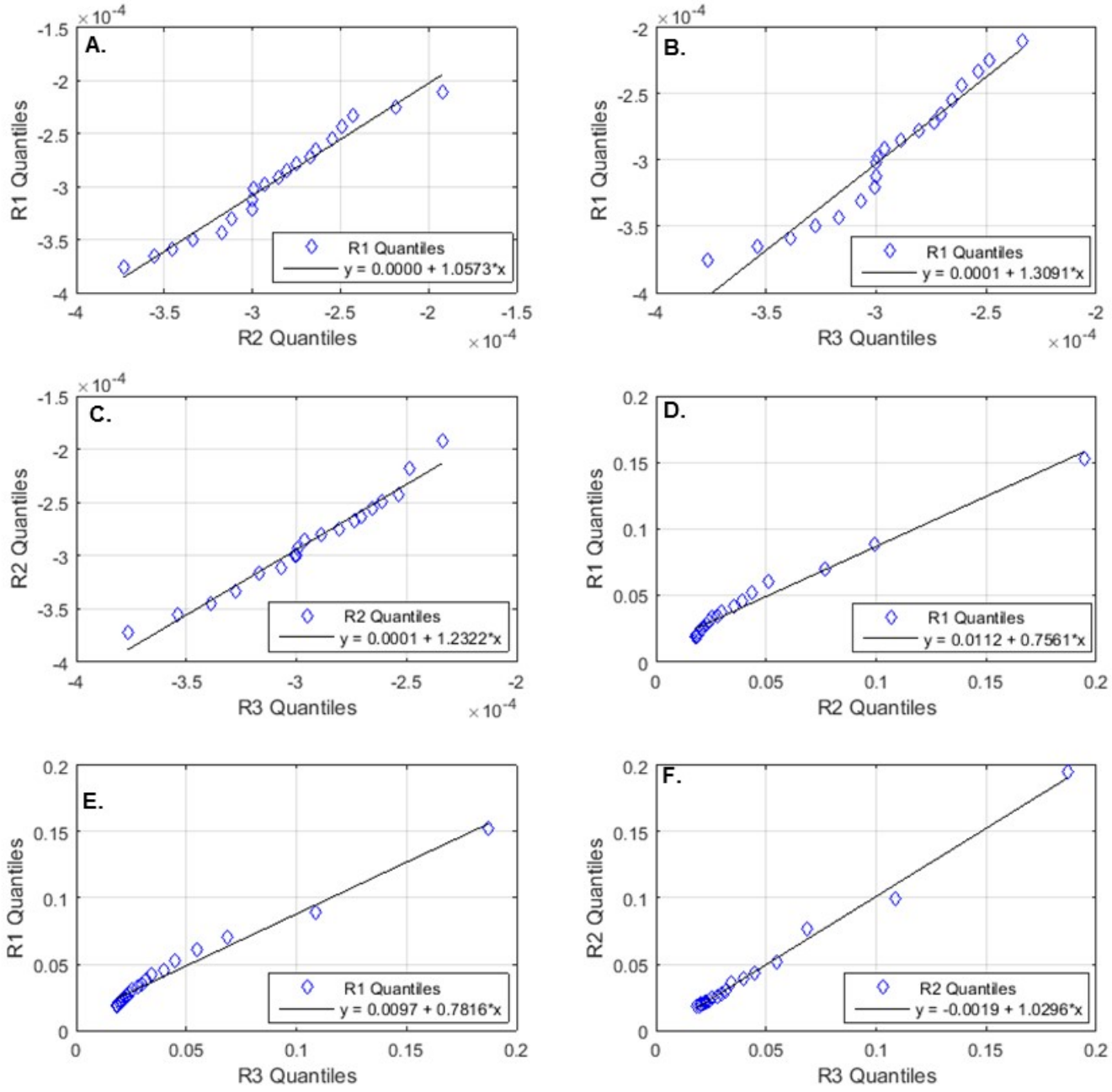

Supplementary Figure 7. Linear regression analysis of QQ data of murine liver autophagy organelles labeled with 50nM DyLight488-conjugated anti-LC3 antibody. (A-C). Linear regressions between quantiles of electrophoretic mobility distributions of pairs of replicates. From (A) to (C), the 95% confidence intervals for the slope of each comparison were [1.0 1.2], [1.2 1.5], [1.1 1.2], respectively; the slopes were not statistically different (p=0.05). (D-F). Linear regressions between quantiles of intensity distributions of pairs of replicates. From (D) to (F), the 95% confidence intervals for the slope of each comparison were [0.7, 0.8], [0.7 0.8], and [1.0, 1.1], respectively; the slopes were statistically different (p=0.05). Replicate 1 (R1), Replicate 2 (R2), Replicate 3 (R3) are described in Figure 5 of the main manuscript. Data acquired using conditions described in Figure 1 of the main manuscript.